



The reaction $\bar{p}p \rightarrow \bar{\Lambda}_c^- \Lambda_c^+$ close to threshold

J. Haidenbauer^{a,*}, G. Krein^b

^a Institute for Advanced Simulation and Jülich Center for Hadron Physics, Forschungszentrum Jülich, D-52425 Jülich, Germany

^b Instituto de Física Teórica, Universidade Estadual Paulista, Rua Dr. Bento Teobaldo Ferraz, 271-01140-070 São Paulo, SP, Brazil

ARTICLE INFO

Article history:

Received 16 December 2009
 Received in revised form 26 January 2010
 Accepted 19 March 2010
 Editor: J.-P. Blaizot

Keywords:

Charmed-baryon production
 Proton–antiproton annihilation
 Meson-exchange model
 Quark model

ABSTRACT

Predictions for the charm-production reaction $\bar{p}p \rightarrow \bar{\Lambda}_c^- \Lambda_c^+$ for energies near the threshold are presented. The calculations are performed in a meson-exchange framework in close analogy to our earlier study on $\bar{p}p \rightarrow \bar{\Lambda} \Lambda$ by connecting the two processes via $SU(4)$ symmetry. The obtained $\bar{\Lambda}_c^- \Lambda_c^+$ production cross sections are in the order of 1 to 7 μb , i.e. a factor of around 10–70 smaller than the corresponding cross sections for $\bar{\Lambda} \Lambda$. However, they are 100 to 1000 times larger than predictions of other model calculations in the literature.

© 2010 Elsevier B.V. All rights reserved.

1. Introduction

The study of the production of charmed hadrons in antiproton–proton ($\bar{p}p$) collisions is of importance for the understanding of the strong force in the non-perturbative regime of QCD. The FAIR project at the GSI laboratory has an extensive program aiming at a high-accuracy spectroscopy of charmed hadrons and at an investigation of their interactions with ordinary matter [1]. Presently little is known about such interactions, yet their knowledge is a prerequisite for investigating issues like in-medium properties of charmed hadrons, e.g. $c\bar{c}$ -quarkonium dissociation and changes in properties of D mesons due to chiral symmetry restoration effects on the light quarks composing these mesons. Therefore there is an urgent need for theoretical investigations to guide such experiments.

In the present Letter we concentrate on the reaction $\bar{p}p \rightarrow \bar{\Lambda}_c^- \Lambda_c^+$ close to its threshold. Providing predictions or simply estimations for this reaction is very challenging. First of all, the lack of any direct empirical information on this reaction makes it difficult to constrain model parameters. Second, both long-distance and short-distance physics are present in the reaction and this poses the question on the appropriate degrees of freedom to be used in order to describe it, quarks and gluons or mesons and baryons, or a combination of both. To the best of our knowledge, presently there are only four elaborate studies that consider this

reaction. The most recent publication is by Goritschnig et al. [2], who employ a quark–gluon description based on a factorization hypothesis of hard and soft processes. This work supersedes an earlier study by that group within a quark–diquark picture, where already concrete predictions for the $\bar{\Lambda}_c^- \Lambda_c^+$ production cross section were given [3]. In the study by Kaidalov and Volkovitsky [4] a non-perturbative quark–gluon string model is used, based on secondary Regge pole exchanges including absorptive corrections. On the same lines, there is the more recent publication by Titov and Kämpfer [5].

Our work here builds on the Jülich meson–baryon model [6,7] for the reaction $\bar{p}p \rightarrow \bar{\Lambda} \Lambda$. In that model the hyperon-production reaction is considered within a coupled-channel approach. This allows to take into account rigorously the effects of the initial ($\bar{p}p$) and final ($\bar{\Lambda} \Lambda$) state interactions which play an important role for energies near the production threshold [6–9]. The microscopic strangeness production process and the elastic parts of the interactions in the initial ($\bar{p}p$) and final ($\bar{\Lambda} \Lambda$) states are described by meson exchanges, while annihilation processes are accounted for by phenomenological optical potentials. The elastic parts of the initial- and final-state interactions (ISI and FSI) are G -parity transforms of an one-boson-exchange variant of the Bonn NN potential [10] and of the hyperon–nucleon model A of Ref. [11], respectively. The model achieved a reasonably good overall description of the wealth of $\bar{p}p \rightarrow \bar{\Lambda} \Lambda$ data collected by the P185 Collaboration at LEAR (CERN) on total and differential cross sections and spin observables [12] – see also the review in Ref. [13].

The extension of the model to the charm sector here follows a strategy similar to our recent work on the DN and $\bar{D}N$ interactions

* Corresponding author.

E-mail address: j.haidenbauer@fz-juelich.de (J. Haidenbauer).

[14,15], which used the original Jülich meson-exchange model for the KN system [16,17] and improvements from quark–gluon dynamics at short distances [18,19]. Specifically, in the present Letter we construct an extension of the meson-exchange model of Refs. [6,7] to the reaction $\bar{p}p \rightarrow \bar{\Lambda}_c^- \Lambda_c^+$ assuming as a working hypothesis $SU(4)$ symmetry constraints. We examine the sensitivity of the results to changes in the elastic and annihilation parts of the initial $\bar{p}p$ interaction and inspect the effects of the final $\bar{\Lambda}_c^- \Lambda_c^+$ interaction and of the form factors that enter in the $\bar{p}p \rightarrow \bar{\Lambda}_c^- \Lambda_c^+$ transition potential described by t -channel D and D^* meson exchanges. In addition, we also investigate the effect of replacing this meson-exchange transition by a charm-production potential derived in a quark model. We believe this is important for assessing uncertainties in the model, since one could easily raise the question on the validity of a meson-exchange description of the transition in view of the large masses of the exchanged mesons.

In the next section we discuss the basic ingredients of the model and fix parameters by fitting differential and total inclusive $\bar{p}p$ cross sections. In Section 3 we present numerical results for our predictions for differential and total cross sections and compare with the results available in the literature. A summary of our work is presented in Section 4.

2. The model

We will start discussing the basic ingredients of the original Jülich coupled-channel approach [6,7] that we employ here for the reaction $\bar{p}p \rightarrow \bar{\Lambda}_c^- \Lambda_c^+$. The transition amplitude is obtained from the solution of a coupled-channel Lippmann–Schwinger equation,

$$T(\mathbf{q}', \mathbf{q}, z) = V(\mathbf{q}', \mathbf{q}, z) + \int d^3q'' V(\mathbf{q}', \mathbf{q}'', z) G_0(\mathbf{q}'', z) T(\mathbf{q}'', \mathbf{q}, z), \quad (1)$$

where z is the initial energy and \mathbf{q}' (\mathbf{q}) the c.m. (center-of-mass) relative momentum in the initial (final) state. Here V is a 2×2 matrix in channel space containing the interaction potentials (channel 1 = $p\bar{p}$, channel 2 = $\bar{\Lambda}_c^- \Lambda_c^+$)

$$V(\mathbf{q}', \mathbf{q}, z) = \begin{pmatrix} V^{11}(\mathbf{q}', \mathbf{q}, z) & V^{12}(\mathbf{q}', \mathbf{q}, z) \\ V^{21}(\mathbf{q}', \mathbf{q}, z) & V^{22}(\mathbf{q}', \mathbf{q}, z) \end{pmatrix}, \quad (2)$$

and $G_0(\mathbf{q}, z)$ is the propagator

$$G_0(\mathbf{q}, z) = \begin{pmatrix} 1/(z - E_{\mathbf{q}}^{(1)} + i\epsilon) & 0 \\ 0 & 1/(z - E_{\mathbf{q}}^{(2)} + i\epsilon) \end{pmatrix}, \quad (3)$$

with $E_{\mathbf{q}}^{(1)} = E_{\mathbf{q}}(p) + E_{\mathbf{q}}(\bar{p})$ and $E_{\mathbf{q}}^{(2)} = E_{\mathbf{q}}(\Lambda_c) + E_{\mathbf{q}}(\bar{\Lambda}_c)$. The diagonal potentials V^{ii} are given by the sum of an elastic part and an annihilation part.

Though the Jülich group has developed rather sophisticated models of the NN interaction [20,21] these potentials cannot be used anymore at such high energies. Indeed, already in the study of $\bar{p}p \rightarrow \bar{\Lambda}\Lambda$ the elastic part of the $\bar{N}N$ potential was deduced (via G -parity transform) from a simple, energy-independent one-boson-exchange NN potential (OBEPF) and a phenomenological spin-, isospin-, and energy-independent optical potential of Gaussian form,

$$V_{opt}^{\bar{p}p \rightarrow \bar{p}p}(r) = (U_0 + iW_0)e^{-r^2/2r_0^2}, \quad (4)$$

was added in order to take into account annihilation. Now, at even much higher energies, any NN potential has to be considered as being purely phenomenological. Still we keep the longest ranged (and model-independent) part of the elastic $\bar{p}p$ interaction, namely one-pion exchange. To it we add again an optical potential of the

Table 1

Parameters of the phenomenological optical potential in the $\bar{p}p$ channel for the four different models described in the text.

	A	B	C	D
U_0	−48.0 MeV	100.5 MeV	72.9 MeV	1808 MeV
W_0	−531.9 MeV	−529.5 MeV	−448.3 MeV	−1644 MeV
r_0	0.56 fm	0.56 fm	0.58 fm	0.41 fm

Table 2

Integrated $\bar{p}p$ cross sections at $p_{lab} = 10.1$ GeV/c for the four models considered. The experimental value for the charge-exchange channel $\bar{p}p \rightarrow \bar{n}n$ (cex) is for $p_{lab} = 9$ GeV/c [24].

	σ_{tot} (mb)	σ_{el} (mb)	σ_{cex} (mb)
Experiment	54.7 ± 0.60 [22]	14.6 ± 3.3 [23]	0.284 ± 0.041 [24]
A	54.2	14.4	0.20
B	54.1	14.6	0.23
C	54.3	14.2	0.42
D	54.6	20.6	2.82

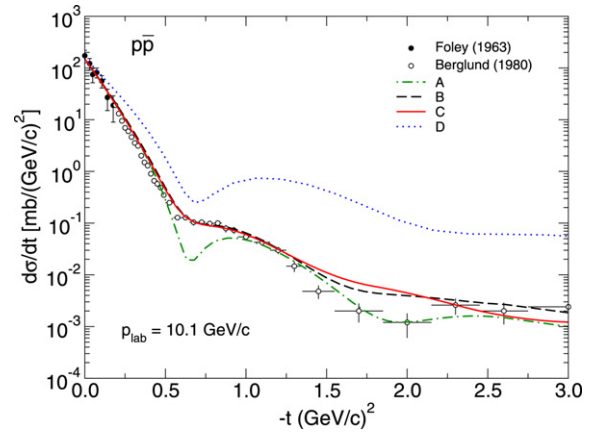


Fig. 1. Differential cross section for elastic $\bar{p}p$ scattering at $p_{lab} = 10.1$ GeV/c as a function of t . The dash-dotted curve corresponds to a calculation where only one pion exchange is added to the optical potential (A). The dotted curve results when the complete G -parity transformed OBEPF model of Ref. [10] is used for the elastic part (D). The dashed and solid curves are obtained by leaving out vector-meson exchanges (B) or by reducing the elastic part (except for the pion exchange) to 10% (C), respectively. The experimental information is taken from Foley et al. [23] and Berglund et al. [25].

form given in Eq. (4) and determine the parameters (U_0 , W_0 , r_0 , cf. Table 1) by a fit to $\bar{N}N$ data in the energy range relevant for the reaction $\bar{p}p \rightarrow \bar{\Lambda}_c^- \Lambda_c^+$. Fortunately, there are total cross sections [22–24] and even differential cross sections [23,25] around $p_{lab} = 10$ GeV/c, i.e. fairly close to the $\bar{\Lambda}_c^- \Lambda_c^+$ threshold which is at 10.162 GeV/c. This $\bar{p}p$ potential is called model A in the following. As can be seen from Table 2 and Fig. 1 the integrated cross sections as well as the $\bar{p}p$ differential cross section are fairly well reproduced.

One knows from studies on $\bar{p}p \rightarrow \bar{\Lambda}\Lambda$ that the magnitude of the cross sections depends very sensitively on the ISI [6–9]. Specifically, the absorptive character of the $\bar{N}N$ interaction leads to a strong reduction of the cross section as compared to results obtained in Born approximation, i.e. based on the transition potential alone. Because of that we consider here several variants of the $\bar{N}N$ potential. First, we take the full G -parity transformed OBEPF interaction and add again the optical potential (model D). Obviously in this case, only the total cross section can be still brought in line with the experiment by adjusting the parameters of the optical potential, while all other cross sections are strongly overestimated. Still we consider this potential too with the intention that it serves as an illustration for the uncertainties in our predictions due to

the used $\bar{p}p$ interaction. Realizing that the overestimation of the cross sections is primarily caused by the vector-meson exchange (ρ , ω) contributions [26] to OBEPF, we prepare two more potentials where we (i) leave out those vector mesons altogether (B) or (ii) reduce the elastic part (except for one-pion exchange) to 10% (C). Within both scenarios a rather satisfying description of the $\bar{N}N$ data around 10 GeV/c can be obtained, cf. Table 2 and Fig. 1. In particular, not only the slope but even the shoulder in the differential cross section is reproduced quantitatively by these two interactions.

The interaction in the final $\bar{\Lambda}_c^- \Lambda_c^+$ system is assumed to be the same as the one in $\bar{\Lambda}\Lambda$. Specifically, this means that the elastic part of the interaction is given by the isospin-zero σ and ω exchanges with coupling constants taken from the hyperon–nucleon model A of Ref. [11], while the annihilation part is again parameterized by an optical potential which contains, however, spin-orbit and tensor components in addition to a central component [6]:

$$V_{opt}^{\bar{\Lambda}_c^- \Lambda_c^+ \rightarrow \bar{\Lambda}_c^- \Lambda_c^+}(r) = [U_c + iW_c + (U_{LS} + iW_{LS})\mathbf{L} \cdot \mathbf{S} + (U_t + iW_t)\boldsymbol{\sigma}_{\Lambda_c} \cdot \mathbf{r}\boldsymbol{\sigma}_{\bar{\Lambda}_c} \cdot \mathbf{r}]e^{-r^2/2r_0^2}. \quad (5)$$

The free parameters in the optical $\bar{\Lambda}\Lambda$ potential were determined in Ref. [6] by a fit to data on total and differential cross sections, and analyzing power for $\bar{p}p \rightarrow \bar{\Lambda}\Lambda$. Clearly, there are no reasons to believe that the $\bar{\Lambda}_c^- \Lambda_c^+$ interaction will be the same on a quantitative level. But we expect that at least the bulk properties are similar. Specifically, in both cases near threshold the interactions will be governed by strong annihilation processes. We will investigate the role played by the FSI for our results by simply switching it off. We use the parameters as given in Table 2 of Ref. [7].

In principle, the parameters of $V_{opt}^{\bar{p}p \rightarrow \bar{p}p}$ can only be determined together with those for $\bar{\Lambda}_c^- \Lambda_c^+$ because we consider a coupled-channels problem. However, like in $\bar{\Lambda}\Lambda$ the branching ratio $\bar{p}p \rightarrow \bar{\Lambda}_c^- \Lambda_c^+$ is so small that the effect of the $\bar{\Lambda}_c^- \Lambda_c^+$ channel on the diagonal $\bar{p}p$ T -matrix can be safely neglected.

The transition potential from $\bar{p}p$ to $\bar{\Lambda}_c^- \Lambda_c^+$ is given by t -channel D and D^* exchanges and their explicit expressions are the same as for K and K^* as given in Ref. [11]. They are of the generic form

$$V^{p\bar{p} \rightarrow \bar{\Lambda}_c^- \Lambda_c^+}(t) \sim \sum_{M=D, D^*} g_{N\Lambda_c M}^2 \frac{F_{N\Lambda_c M}^2(t)}{t - m_M^2}, \quad (6)$$

where $g_{N\Lambda_c M}$ are coupling constants and $F_{N\Lambda_c M}^2(t)$ are form factors. Under the assumption of $SU(4)$ symmetry the coupling constants are the same as in the corresponding exchanges in $\bar{p}p \rightarrow \bar{\Lambda}\Lambda$. However, the cutoff masses in the vertex form factors cannot be taken over, because the masses of the exchanged particles are now much larger. We use here a monopole form factor with a cutoff mass Λ of 3 GeV, at the $N\Lambda_c D$ as well as at the $N\Lambda_c D^*$ vertex but we will explore the sensitivity of the results to variations of the cutoff mass.

To examine further the uncertainties, as an alternative we consider here also a charm-production potential inspired by quark-gluon dynamics. There is a large literature associated with strange-hadron production in $p\bar{p}$ reactions, the best known works are those of Kohno and Weise [8], Furui and Faessler [27], Burkardt and Dillig [28], Roberts [29] and Alberg et al. [9] – a more complete list of references can be found in the review of Ref. [13]. In the present study we adopt the interaction proposed by Kohno and Weise, derived in the so-called 3S_1 mechanism of a constituent quark model. In this model the $s\bar{s}$ pair in the final state is created from an initial $u\bar{u}$ or $d\bar{d}$ pair via s -channel gluon exchange. After

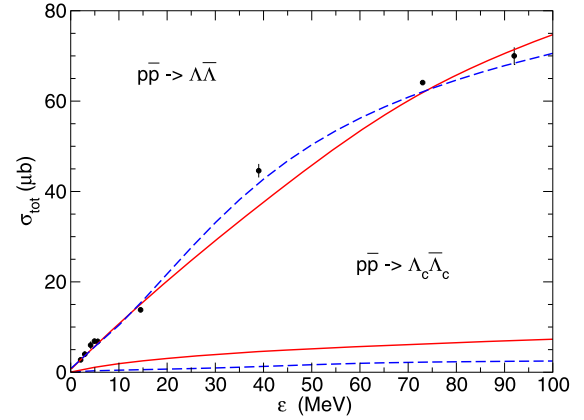


Fig. 2. Total reaction cross sections for $\bar{p}p \rightarrow \bar{\Lambda}\Lambda$ and $\bar{p}p \rightarrow \bar{\Lambda}_c^- \Lambda_c^+$ as a function of the excess energy ϵ . The results for $\bar{p}p \rightarrow \bar{\Lambda}\Lambda$ (upper curves) are taken from our work [7]. The solid curves are results for the meson-exchange transition potential while the dashed curves correspond to quark-gluon dynamics. The $\bar{p}p \rightarrow \bar{\Lambda}_c^- \Lambda_c^+$ results are obtained with the $\bar{p}p$ interaction C. The experimental information is taken from Ref. [12].

quark degrees-of-freedom are integrated out the potential has the form [8]:

$$V^{\bar{p}p \rightarrow \bar{\Lambda}\Lambda}(r) = \frac{4}{3} 4\pi \frac{\alpha}{m_G^2} \delta_{S1} \delta_{T0} \left(\frac{3}{4\pi \langle r^2 \rangle} \right)^{3/2} \times \exp(-3r^2/(4\langle r^2 \rangle)). \quad (7)$$

Here α/m_G^2 is an effective (quark-gluon) coupling strength, $\langle r^2 \rangle$ is the mean square radius associated with the quark distribution in the p or Λ , and S and T are the total spin and isospin in the $\bar{p}p$ system. This simple potential has actually a very modern form, namely that of a contact term, though smeared out by the quark distribution. The effective coupling strength is practically a free parameter that was fixed by a fit to the $\bar{p}p \rightarrow \bar{\Lambda}\Lambda$ data [7]. But it depends implicitly on the effective gluon propagator, i.e. on the square of the energy transfer from initial to final quark pair, cf. Refs. [27,28,30]. Heuristically this energy transfer corresponds roughly to the masses of the produced constituent quarks, i.e. $m_G \approx 2m_q$. Thus, we expect the effective coupling strength α/m_G^2 for charm production to be reduced by the ratio of the constituent quark masses of the strange and the charmed quark squared, $(m_s/m_c)^2 \approx (550 \text{ MeV}/1600 \text{ MeV})^2 \approx 1/9$ as compared to the one for $\bar{p}p \rightarrow \bar{\Lambda}\Lambda$. Note that a different suppression factor arises for the 3P_0 quark-antiquark annihilation vertex, considered by Alberg et al. in their study of $\bar{p}p \rightarrow \bar{\Lambda}\Lambda$ [9]. In this case the amplitude scales with $1/m_q$ so that the effective strength of the transition potential is reduced by $m_s/m_c \approx 1/3$ only when going from strangeness to charm production.

3. Results

Our predictions for the total reaction cross section for $p\bar{p} \rightarrow \bar{\Lambda}_c^- \Lambda_c^+$ are presented in Fig. 2. The cross section is shown as a function of the excess energy $\epsilon = \sqrt{s} - m_{\Lambda_c} - m_{\bar{\Lambda}_c}$ so that we can compare it with the one for $p\bar{p} \rightarrow \bar{\Lambda}\Lambda$ at the corresponding ϵ . The curve in Fig. 2 corresponds to the $\bar{p}p$ model C, for which we obtained the largest results.

Obviously, and as expected, the cross section for $\bar{\Lambda}_c^- \Lambda_c^+$ production is smaller than the one for $\bar{\Lambda}\Lambda$. But the difference is about one order of magnitude only. Indeed, one can understand the reduction qualitatively just by considering the following: When going from $\bar{\Lambda}\Lambda$ to $\bar{\Lambda}_c^- \Lambda_c^+$ within the meson-exchange picture the main change occurs in the meson propagators of the transition

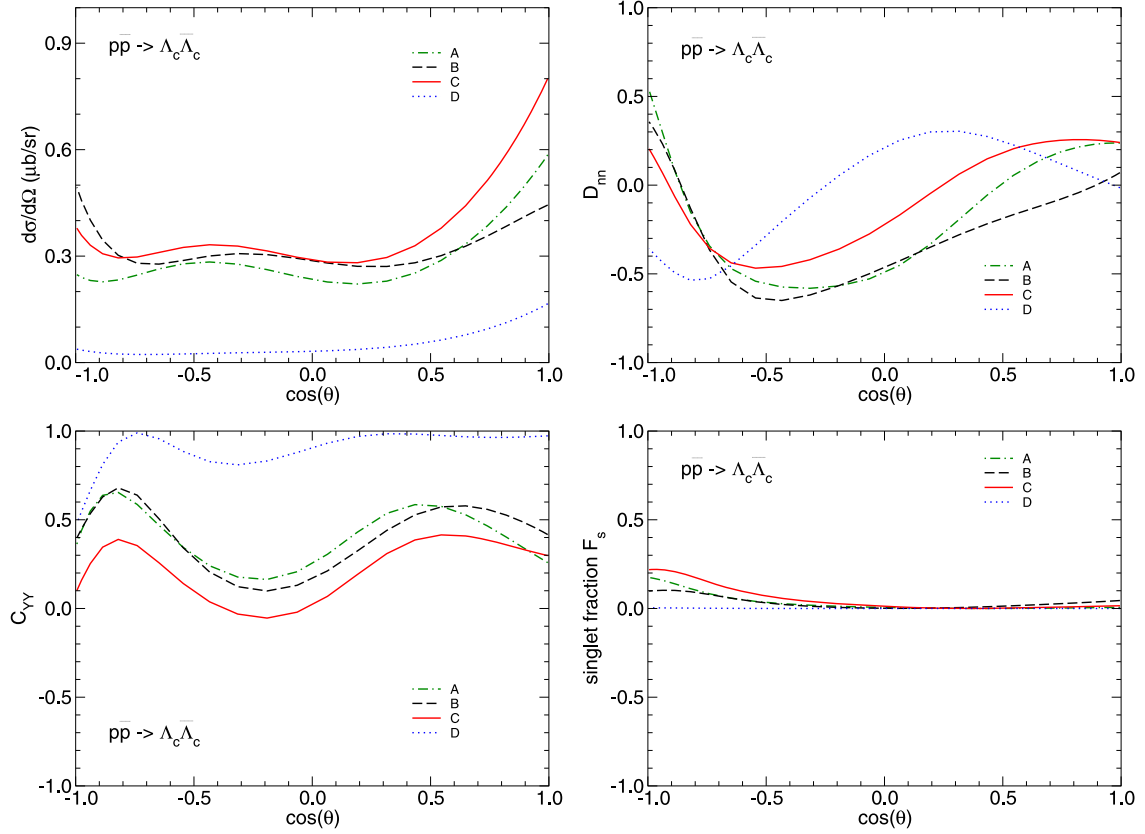


Fig. 3. Differential cross section, singlet fraction, depolarization D_m and spin-correlation parameter C_{yy} for $\bar{p}p \rightarrow \bar{\Lambda}_c \Lambda_c^+$ at $p_{lab} = 10.343$ GeV/ c ($\epsilon = 40$ MeV) as a function of the c.m. scattering angle. The curves correspond to different ISI as indicated in the figure. The meson-exchange potential is used for the transition interaction.

potentials where the masses of the strange mesons (K , K^*) are replaced by those of the charmed mesons (D , D^*), $m_{M_s} \rightarrow m_{M_c}$, cf. Eq. (6). All coupling constants remain the same because of the assumed $SU(4)$ symmetry. Thus, the ratio of the transition potentials is then given roughly by $V^{\bar{p}p \rightarrow \bar{\Lambda}_c \Lambda_c^+} / V^{\bar{p}p \rightarrow \bar{\Lambda} \Lambda} \approx m_{M_s}^2 / m_{M_c}^2 \approx 1/4$ so that one expects the cross section to be smaller by a factor of around 16. Our result is pretty much in line with this admittedly rather qualitative estimation. Of course, in the explicit calculation the situation is much more complex. For example, the t dependence in the propagator and in the form factor (Eq. (6)) induces a somewhat stronger reduction than the one suggested solely by the mass ratio. On the other hand, since the $\bar{N}N$ cross section at the $\bar{\Lambda}_c \Lambda_c^+$ threshold is already significantly smaller than at the $\bar{\Lambda} \Lambda$ threshold, there is less reduction due to the ISI.

Let us now discuss the sensitivity of the results to the various ingredients of our model calculation. The most crucial component is certainly the $\bar{p}p$ interaction in the initial state. Without it, and specifically in Born approximation, we would get cross sections that are more than a factor 100 larger. This is no surprise because the very same gross overestimation in the Born approximation occurs for $\bar{p}p \rightarrow \bar{\Lambda} \Lambda$ [6–9] but also for other exclusive $\bar{p}p$ annihilation channels like $\bar{p}p \rightarrow \pi\pi$, $\bar{p}p \rightarrow K\bar{K}$, etc. [20,21], if one does not take into account the ISI. However, with the ISI included, it is reassuring to see that the variations of the predicted $\bar{p}p \rightarrow \bar{\Lambda}_c \Lambda_c^+$ cross section for the different $\bar{p}p$ potentials we have prepared is fairly small. To be concrete, the cross sections at $\epsilon = 100$ MeV are 5.8, 6.3, and 7.3 μb for the interactions A, B, and C, respectively. Only the result based on the full G -parity transformed OBEPF potential differs more significantly. Here we get a cross section that is with 0.8 μb a factor 10 smaller than the other values. The suppression for this $\bar{p}p$ model is presumably due to the fact that it

yields a $\bar{p}p$ elastic cross section that is much larger than the ones of the other potentials considered, and actually in disagreement with experimental information. Still, the variation of one order of magnitude may be considered as a realistic estimation of the uncertainty due to the ISI.

Once the ISI is included our results turned out to be rather insensitive to the final $\bar{\Lambda}_c \Lambda_c^+$ interaction. Even when we leave it out altogether the cross sections do not change (decrease) by more than 10–15%. We also considered variations of the cutoff mass at the $N\Lambda_c D$ and $N\Lambda_c D^*$ vertices. For the results discussed above a value of $\Lambda = 3$ GeV has been used. When reducing this value to 2.5 GeV the cross sections at $\epsilon = 100$ MeV drop by roughly a factor 3. Of course, employing even smaller cutoff masses would further decrease the cross sections. However, since the exchanged mesons have a mass of around 1.9 to 2 GeV we consider values below 2.5 GeV as being not really realistic.

We display here also the results based on an adaption of the 3S_1 quark-gluon transition mechanism of Ref. [8]. We scale the effective coupling strength $\alpha/m_c^2 = 0.25$ fm 2 , fixed in our study of $\bar{p}p \rightarrow \bar{\Lambda} \Lambda$ [7], with $(m_c/m_s)^2$ using the constituent quark masses $m_s = 550$ MeV and $m_c = 1600$ MeV, i.e. the same values as employed in our previous works in Refs. [14,15]. As expected, we obtain cross sections that are of the same magnitude as those predicted in the meson-exchange picture though roughly a factor three smaller, cf. the dashed line in Fig. 2. In principle the factor $\langle r^2 \rangle$ in Eq. (7) also changes when replacing m_s by m_c , since it gives the size of the quark distribution of the overlapping hadrons – $\langle r^2 \rangle$ decreases as m_s is replaced by m_c . We have not changed this factor in the present work, since we expect this change to be much smaller than the change in the square of the energy transfer m_c^2 , since hadron sizes do not scale as simple powers of quark masses

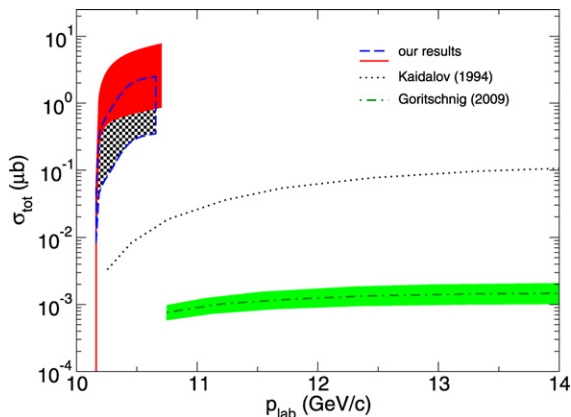


Fig. 4. Total reaction cross sections for $\bar{p}p \rightarrow \bar{\Lambda}_c^- \Lambda_c^+$ as a function of the laboratory momentum p_{lab} . The dark (red) shaded band (blue grid) is the prediction of our meson-exchange (quark-gluon) transition potential. The dotted curve is the result from Ref. [4] while the dash-dotted curve and the corresponding (green) band are from Ref. [2]. (For interpretation of the references to colour in this figure legend, the reader is referred to the web version of this Letter.)

and so the overlap between hadron wave functions is not expected to change drastically from Λ to Λ_c – for explicit numbers for the size parameters of harmonic oscillator wave functions for N and Λ_c see Ref. [31]. The size parameter we use is $\langle r^2 \rangle^{1/2} = 0.55$ fm.

Predictions for differential cross sections, the singlet fraction F_s , the depolarization D_{nn} and the spin-correlation parameter C_{yy} (cf. Ref. [7] for definitions) at $\epsilon = 40$ MeV are presented in Fig. 3 for all four ISI considered. Note that the singlet fraction is defined by $F_s = \frac{1}{4}(1 - \langle \vec{\sigma}_1 \cdot \vec{\sigma}_2 \rangle) = \frac{1}{4}(1 + C_{xx} - C_{yy} + C_{zz})$ [6]. It is zero if the $\bar{\Lambda}_c^- \Lambda_c^+$ pair is produced purely in a triplet state. Indeed in case of $\bar{p}p \rightarrow \bar{\Lambda}\Lambda$ it was found experimentally that the singlet fraction is close to zero [12] and this feature was reproduced by meson-exchange potentials [6] as well as by transition interactions based on quark-gluon dynamics [7–9]. In the former it is due to a strong tensor force generated by the combined $K + K^*$ exchange which leads to a dominance of transitions of the form $L_{\bar{\Lambda}\Lambda} = L_{\bar{p}p} - 2$ where L refers to the orbital angular momentum. As can be seen from Fig. 3, the very same feature is predicted also for the reaction $\bar{p}p \rightarrow \bar{\Lambda}_c^- \Lambda_c^+$. The differential cross section exhibits a peak in forward direction, similar to what has been also observed for $\bar{p}p \rightarrow \bar{\Lambda}\Lambda$ [6,7,12].

Let us now compare our predictions with those by other groups. This is done in Fig. 4. Goritschnig et al. [2] as well as Kaidalov and Volkovitsky [4] have presented explicit results in their publications and we reproduce them in Fig. 4 to facilitate a comparison. Our results are shown as dark (red) shaded band (and grid) in order to reflect the variation of the predictions when the four different ISI are used. It is remarkable that our results differ drastically from those of the preceding works. Specifically, our cross sections are a factor 1000 larger than those given by Goritschnig et al. and they are still about 100 times larger than the ones by Kaidalov and Volkovitsky. Thus, even when considering the variation of about a factor ten due to the ISI that we see in our results and the uncertainties due to the unconstrained FSI and form factors in the transition potential that amount to roughly a factor three, we are faced with an impressive qualitative difference.

4. Summary

In this Letter we presented predictions for the charm-production reaction $\bar{p}p \rightarrow \bar{\Lambda}_c^- \Lambda_c^+$. The calculations were performed in the meson-exchange framework in close analogy to our earlier study on $\bar{p}p \rightarrow \bar{\Lambda}\Lambda$ by connecting the two processes via $SU(4)$ symmetry. The interaction in the initial $\bar{p}p$ interaction, which plays

a crucial role for the quantitative predictions and which is now needed at a much higher energy, is re-adjusted so that available $\bar{p}p$ scattering data in the relevant energy range are reproduced.

The obtained $\bar{\Lambda}_c^- \Lambda_c^+$ production cross sections are in the order of 1 to 7 μb . Thus, they are just about a factor 10–70 smaller than the corresponding cross sections for $\bar{\Lambda}\Lambda$. The reduction is in line with a naive estimation based on the mass ratio of strange (K, K^*) versus charmed (D, D^*) mesons. The exchange of those mesons governs the range of the forces that are responsible for producing a Λ or a Λ_c , respectively, in the meson-exchange picture.

Since one could question the validity of a meson-exchange description of the charm-production process in view of the large masses of the exchanged mesons we investigated the effect of replacing this meson-exchange transition by a production potential derived in a quark model. It was reassuring to see that within both pictures we arrive at predictions of essentially the same order of magnitude. Thus, what seems to matter are not the details of the production mechanism but the involved scales and these are determined by the masses of the exchanged mesons or, equivalently, the constituent masses of the charm quark.

Interestingly, other model calculations in the literature predict $\bar{\Lambda}_c^- \Lambda_c^+$ production cross sections that are 100 to 1000 times smaller than what we found. Since the approaches used in those calculations are rather different from ours it is practically impossible to say where this drastic difference in the predicted cross sections comes from. Hence, a discrimination between those scenarios appears to be possible only when the reaction $\bar{p}p \rightarrow \bar{\Lambda}_c^- \Lambda_c^+$ will be examined in a future experiment at FAIR. Of course, if our predictions turn out to be closer to reality than the others, it will be much easier to perform a pertinent experiment at FAIR. Moreover, Λ_c 's and $\bar{\Lambda}_c$'s can then be produced more copiously so that also any other experiment that requires charmed baryons as a probe will be much more promising.

The model presented here leaves room for improvements in several directions. In particular, it would be important to extend the simple picture of s -channel $q\bar{q}$ annihilation followed by $c\bar{c}$ creation for the transition amplitude in the quark model as used here. An interesting possibility is the one pursued in Ref. [29] for $\bar{p}p \rightarrow \bar{\Lambda}\Lambda$ where interacting many-quark intermediate states are considered in the process.

Acknowledgements

We acknowledge stimulating discussions with Tord Johansson and Wolfgang Schweiger on the topic of this Letter. We thank Ulf-G. Meißner for his careful reading of our manuscript. Work partially supported by CNPq and FAPESP (Brazilian agencies).

References

- [1] W. Erni, et al., Panda Collaboration, arXiv:0903.3905 [hep-ex].
- [2] A.T. Goritschnig, P. Kroll, W. Schweiger, Eur. Phys. J. A 42 (2009) 43.
- [3] P. Kroll, B. Quadder, W. Schweiger, Nucl. Phys. B 316 (1989) 373.
- [4] A.B. Kaidalov, P.E. Volkovitsky, Z. Phys. C 63 (1994) 517.
- [5] A.I. Titov, B. Kämpfer, Phys. Rev. C 78 (2008) 025201.
- [6] J. Haidenbauer, T. Hippchen, K. Holinde, B. Holzenkamp, V. Mull, J. Speth, Phys. Rev. C 45 (1992) 931.
- [7] J. Haidenbauer, K. Holinde, V. Mull, J. Speth, Phys. Rev. C 46 (1992) 2158.
- [8] M. Kohno, W. Weise, Phys. Lett. B 179 (1986) 15.
- [9] M.A. Alberg, E.M. Henley, L. Wilets, P.D. Kunz, Nucl. Phys. A 560 (1993) 365.
- [10] J. Haidenbauer, K. Holinde, M.B. Johnson, Phys. Rev. C 45 (1992) 2055.
- [11] B. Holzenkamp, K. Holinde, J. Speth, Nucl. Phys. A 500 (1989) 485.
- [12] P.D. Barnes, et al., Phys. Lett. B 229 (1989) 432;
P.D. Barnes, et al., Nucl. Phys. A 526 (1991) 575;
P.D. Barnes, et al., Phys. Rev. C 54 (1996) 1877.

- [13] E. Klempt, F. Bradamante, A. Martin, J.-M. Richard, *Phys. Rep.* 368 (2002) 119.
- [14] J. Haidenbauer, G. Krein, U.-G. Meißner, A. Sibirtsev, *Eur. Phys. J. A* 33 (2007) 107.
- [15] J. Haidenbauer, G. Krein, U.-G. Meißner, A. Sibirtsev, *Eur. Phys. J. A* 37 (2008) 55.
- [16] R. Büttgen, K. Holinde, A. Müller-Groeling, J. Speth, P. Wyborny, *Nucl. Phys. A* 506 (1990) 586.
- [17] M. Hoffmann, J.W. Durso, K. Holinde, B.C. Pearce, J. Speth, *Nucl. Phys. A* 593 (1995) 341.
- [18] D. Hadjimichef, J. Haidenbauer, G. Krein, *Phys. Rev. C* 66 (2002) 055214.
- [19] J. Haidenbauer, G. Krein, *Phys. Rev. C* 68 (2003) 052201.
- [20] T. Hippchen, J. Haidenbauer, K. Holinde, V. Mull, *Phys. Rev. C* 44 (1991) 1323;
- V. Mull, J. Haidenbauer, T. Hippchen, K. Holinde, *Phys. Rev. C* 44 (1991) 1337.
- [21] V. Mull, K. Holinde, *Phys. Rev. C* 51 (1995) 2360.
- [22] S.P. Denisov, et al., *Nucl. Phys. B* 65 (1973) 1.
- [23] K.J. Foley, et al., *Phys. Rev. Lett.* 11 (1963) 503.
- [24] P. Astbury, et al., *Phys. Lett.* 23 (1966) 160.
- [25] A. Berglund, et al., *Nucl. Phys. B* 176 (1980) 346.
- [26] K.O. Eysler, R. Machleidt, W. Scobel, *Eur. Phys. J. A* 22 (2004) 105.
- [27] S. Furui, A. Faessler, *Nucl. Phys. A* 468 (1987) 699.
- [28] M. Burkardt, M. Dillig, *Phys. Rev. C* 37 (1988) 1362.
- [29] W. Roberts, *Z. Phys. C* 49 (1991) 633.
- [30] M. Kohno, W. Weise, *Phys. Lett. B* 152 (1985) 303.
- [31] J.P. Hilbert, N. Black, T. Barnes, E.S. Swanson, *Phys. Rev. C* 75 (2007) 064907.